CrossMark

In situ Study on the Growth Behavior of Primary Al₃Ni Phase in Solidifying Al–Ni Alloy by Synchrotron Radiography

Si-Yu Sun[1] · Qiao-Dan Hu[1] · Wen-Quan Lu[1] · Zong-Ye Ding[1] · Ming-Qin Xu[1] · Ming-Xu Xia[1] · Jian-Guo Li[1]

Abstract

The growth behavior of Al₃Ni intermetallic compounds (IMCs) during the directional solidification of Al-10 wt% Ni alloy was investigated by synchrotron radiography. Two main growth patterns of primary Al₃Ni phase, I-like and V-like, appeared during solidification, and I-like Al₃Ni phase grew faster than V-like phase, which can be explained by the minimum energy criterion. The growth of I-like phase can be divided into two stages and was mainly affected by undercooling and Ni concentration. We also found that V-like Al₃Ni phase can evolve into M-like phase during solidification.

Keywords Synchrotron radiography · Directional solidification · Intermetallic compounds · Al–Ni alloy

1 Introduction

Al–Ni alloys have been widely used as structural materials due to their low densities, good casting properties and high electrical and thermal conductivity [1, 2]. As Al₃Ni phase is the major intermetallic compound in Al–Ni alloys, and its morphology has significant impact on the strength and performance of casting products [3, 4], the primary Al₃Ni phase in Al–Ni alloys has been studied extensively. For example, Juarez-Hernandez et al. [5] found that Al₃Ni phase aligns typically along the growth direction during the directional solidification of the Al–Ni alloy, and the relationship between its growth temperature and growth velocity agrees well with Hunt-Lu model. Li et al. [6, 7] and Wang et al. [8] concluded that when the magnetic field intensity rises above a critical value, the alignment degree of primary Al₃Ni phase increases with increasing magnetic field intensity. In general, the morphology and alignment behavior of the primary Al₃Ni phase mainly depend on the applied casting conditions.

However, due to opacity and high temperature of alloy melt, the formation of intermetallic compounds (IMCs) is inferred mostly by quenching and dissecting solidified structures [9, 10], sometimes combined with simulations [11], leading to the evolution and dynamics of IMCs poorly understood. Fortunately, the emergence of the synchrotron radiography provides a feasible way to solve the above-mentioned problem. And this imaging technology has been used to observe the growth behavior of Ag₃Sn IMCs in Sn-3.5Ag/Cu interface, by which the competitive growth of different Ag₃Sn growth patterns was recorded throughout the whole process [12]. Also, Huang et al. [13] studied the dissolution and growth of Cu₆Sn₅ IMCs in Sn/Cu solder interconnect, and Puncreobutr et al. [14] studied the growth kinetics of β-Al₅FeSi IMCs during solidification of Al-7.5 Si-3.5 Cu-0.6 Fe (wt%) alloy. Nonetheless, only few attentions have been paid to the growth behavior of Al₃Ni IMCs in solidifying Al–Ni alloy. Very recently, we found that the needle-like IMCs evolve into lamellar phase during cooling at the interface of liquid Al/solid Ni, but we did not focus on the preferred orientation of IMCs [15]. Here, using synchrotron radiography, we obtained in situ X-ray images of the microstructural evolution during the directional solidification of the Al-10 wt% Ni alloy. The

✉ Qiao-Dan Hu
  qdhu@sjtu.edu.cn

[1] Shanghai Key Laboratory of Materials Laser Processing and Modification, School of Materials Science and Engineering, Shanghai Jiao Tong University, Shanghai 200240, China

orientation and growth behaviors of Al$_3$Ni IMCs were uncovered.

2 Experimental Procedure

The Al-10 wt% Ni alloy was melted with pure Al (99.999%) and pure Ni (99.99%) in a high-frequency induction melting furnace and then was cut into sheets with length 14 mm, width 10 mm and thickness 0.5 mm. Specimens were ground, polished and then cleaned ultrasonically before they were directionally solidified. The solidification experiment was carried out in a Bridgman-type furnace at the BL13W1 beam line station of Shanghai Synchrotron Radiation Facility (SSRF). Figure 1 shows the schematic diagram of experimental setup. The sample was fixed upright and sealed by two pieces of Al$_2$O$_3$ plate with the thickness of 0.3 mm. At first, the sample was placed on the top of the field of view where the temperature was set as 800 °C. After holding for 45 min, the sample and Al$_2$O$_3$ plates were pulled down at 3 μm/s with X-ray and view field fixed. The energy of monochromatic beam was selected as 25 keV. A charge-coupled device (CCD) camera that was 80 cm away from the sample was used to collect the images, with a resolution ratio of 3.25 μm/pixel and an exposure time of 500 ms. After the directional solidification experiment, the synchrotron radiation images were manipulated by the Image-Pro Plus 6.0 image analyzer software and the region that contains our research targets was selected. The sizes of the IMCs were calibrated and measured. The morphologies and chemical composition of the sample were obtained by scanning electron microscopy (SEM) equipped with an energy-dispersive spectrometer (EDS), and the phases were determined by X-ray diffraction (XRD).

3 Results and Discussion

Figure 2 shows the microstructural evolution during the directional solidification of Al-10 wt% Ni alloy. The time when the sample began to cool down was set as the initial time (0 s). The solidification process has also been recorded as a video, which can be found in the supplemental material (Supplementary video 1). The top dark gray zone is Al–Ni melt, and the light gray zone at the bottom is ceramic plate. From Fig. 2a, b, few I-like and V-like IMCs with an acute angle appeared during the early stage of solidification. As time prolonged, the I-like IMC (marked in Fig. 2b) grew in two opposite directions and it grew more preferentially from top to bottom (Fig. 2b, c). After it touched the edge of the sample, it could only grow from bottom to up (Fig. 2d–i). Meanwhile, IMCs with I-like and V-like shapes nucleated at different instants and then grew (Fig. 2c–i). Particularly, a V-like IMC evolved into an M-like IMC marked by circles in Fig. 2g–i.

Figure 3a shows the solidified cross-sectional morphology of the IMCs. The cross section is the plane perpendicular to the X-ray path. As described above, mainly two kinds of growth patterns of IMCs were observed. Through the analysis of EDS (Fig. 3b–d) and XRD (Fig. 3e) results, both of them are identified as Al$_3$Ni phase, which are the products of hypereutectic reaction according to the Al–Ni phase diagram [16].

Why the Al$_3$Ni IMCs grow in the forms of I-like and V-like? Al$_3$Ni is an orthorhombic structure, which orientation indexes are <010> = [010], [0$\bar{1}$0] with angle of 180° [17, 18]. As energy densities along the close-packed directions are smaller than those along other directions, crystal grows preferentially along the close-packed directions [12, 19], which contributes to the formation of I-like Al$_3$Ni phase, as illustrated in Fig. 4a.
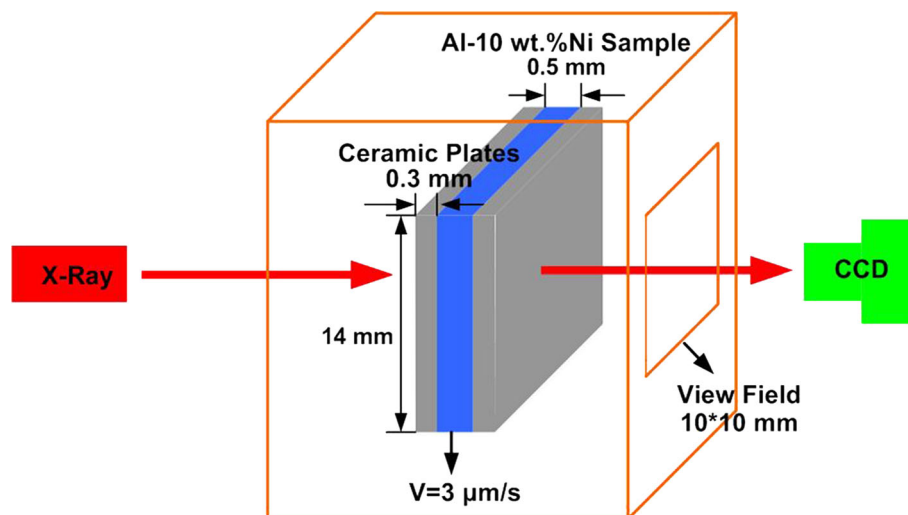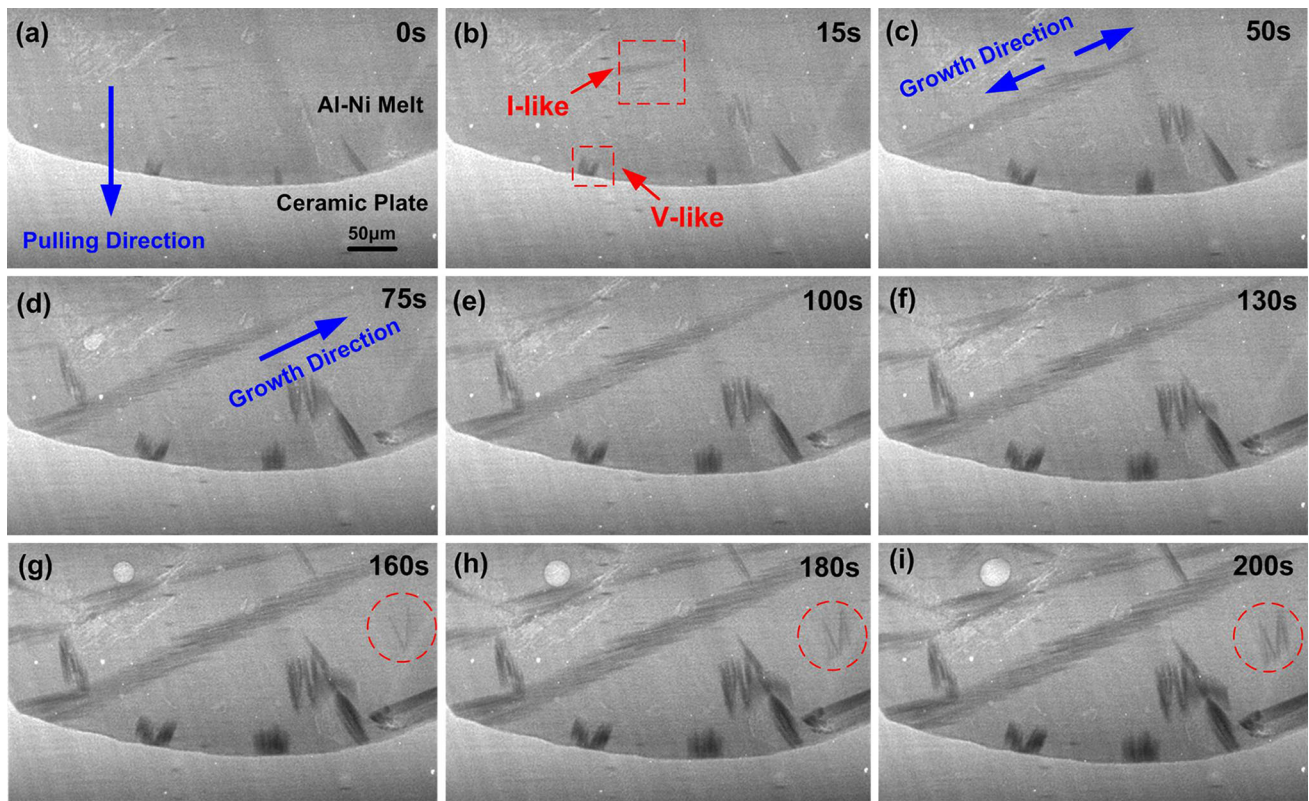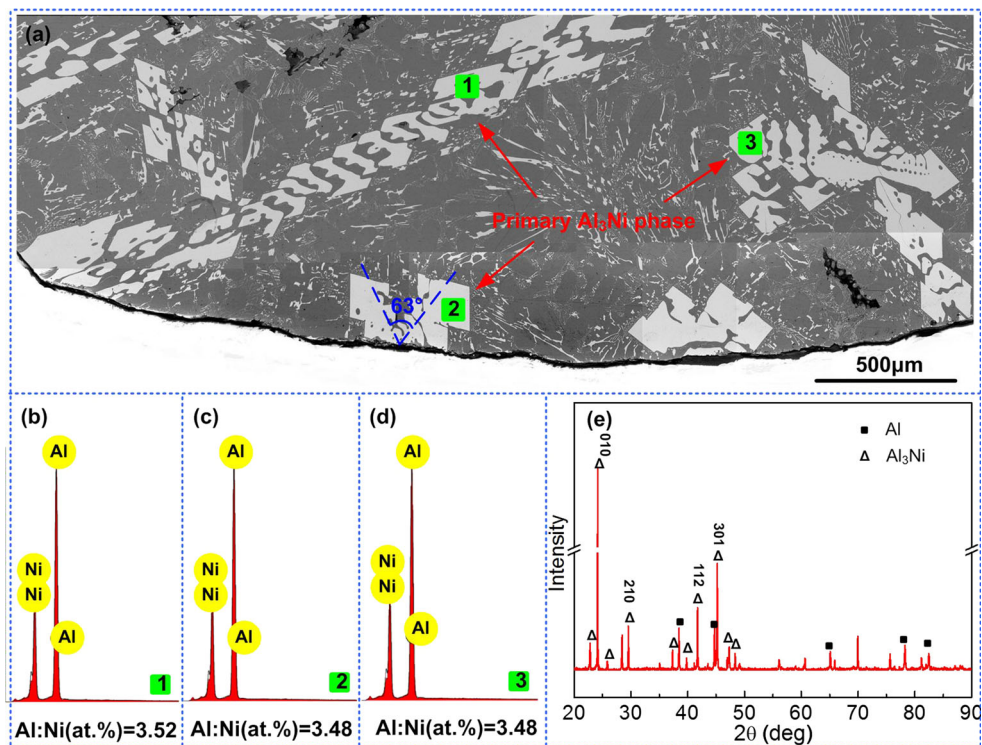

Fig. 1 Schematic diagram of synchrotron radiation experimental configuration

Fig. 2 Synchrotron radiation images of the microstructural evolution during the directional solidification of Al-10 wt% Ni alloy with a pulling rate of 3 μm/s

Fig. 3 a Cross-sectional morphology of the IMCs after solidification; **b–d** composition analysis; **e** XRD pattern of IMCs

Obviously, in contrast to I-like Al$_3$Ni, the two growth orientations of V-like shape have an acute angle approximate 63° as shown in Fig. 3a. According to the XRD result in Fig. 3e, the preferential growth orientation of Al$_3$Ni is <010> which is perpendicular to the first close-packed plane (010), and the other would be perpendicular to the second or third close-packed plane, (301) or (112). After calculation, the angle between <010> and the orientation that is perpendicular to (301) is 90°, and the angle between <010> and the orientation that is perpendicular to (112) is 66°, which is nearly consistent with the X-ray observation (Fig. 2) and SEM (Fig. 3a) results. And the formation mechanism of V-like Al$_3$Ni phase is depicted in Fig. 4b.

To compare the growth behaviors of the two kinds of growth patterns marked in Fig. 2b, the time dependence of their length (L) and width (W) is shown in Fig. 5a, b, respectively. The measuring methods for each kind of shape have been articulated under those curves (For V-like Al$_3$Ni phase, $L = (L_1 + L_2)/2$, and $W = (W_1 + W_2)/2$). It can be seen that I-like Al$_3$Ni phase grew more quickly than V-like Al$_3$Ni phase and achieved a larger size finally. These phenomena can be explained from the following two aspects. First, as mentioned above, from the crystallography viewpoint, <010> crystal direction of the Al$_3$Ni crystal is its preferred growth direction due to its smallest energy density; second, from the nucleation energy viewpoint, the total free energy change (ΔG) of heterogeneous nucleation is expressed as [20]:

$$\Delta G = f(\theta)\left(\sigma 4\pi r^2 + \frac{\Delta g 4\pi r^3}{3}\right), \tag{1}$$

$$f(\theta) = \frac{(2 + \cos\theta)(1 - \cos\theta)^2}{4}, \tag{2}$$

where θ is the wetting angle; σ is specific surface energy; Δg is the Gibbs free energy per unit volume; and r is the radius of nucleus. In the formula, $\frac{\Delta g 4\pi r^3}{3}$ is volume free energy change, which is the driving force of phase change, while $4\pi r^2\sigma$ is surface free energy change, which is the resistance of phase change. For the Al–Ni alloy, I-like

Al$_3$Ni phase has less specific surface area compared with V-like Al$_3$Ni phase, so ΔG of I-like Al$_3$Ni phase is relatively lower and it grew more preferentially. Similarly, it has been reported by Ma et al. [12] that linear Ag$_3$Sn grew up more easily than Y-like and X-like Ag$_3$Sn due to its fewer crystal orientations; Wang et al. [19] also found that I-like Cu$_6$Sn$_5$ with less specific surface area grew more preferentially than Y-like and bird-like ones.

From Fig. 5a, two stages can be easily identified in the length variation curve of the I-like Al$_3$Ni phase: a nearly linear increase in the length in the stage I, followed with a decelerating increase in the length to finally reach a plateau in the stage II. In stage I, the I-like Al$_3$Ni grew in two opposite directions with withdrawal, and it grew more preferentially toward the low-temperature zone because the temperature ahead of the lower tip dropped rapidly and big undercooling existed. After it touched the edge of the sample, it could only grow from bottom to up. Thus, the undercooling decreased, leading to the lower growth rate in stage II. Besides, the decrease in growth rate in stage II can also be ascribed to Ni depletion in nearby Al matrix melt.

It is worth to note that, as shown in Fig. 6, V-like IMC can evolve into M-like IMC, and this process has been recorded as a video, which can be found in the supplemental material (Supplementary video 2). However, it is interesting that the intersection angle of initial V-like IMC is approximately 32° rather than 66° as mentioned above. After calculation, we find that the angle between the orientations that are perpendicular to the second close-packed plane (301) and the fourth close-packed plane (210) is 31.9°, which is in good agreement with the observed value. It may be the fluctuations of temperature and concentration in melt that resulted in the formation and growth of different orientation nucleus. Subsequently, the two tips of the V-like IMC would be new nucleation sites of the Al$_3$Ni phase, and then the newly formed IMCs grow along the pulling direction during solidification to form M-like IMC. Further study is required to provide more information about the temperature and concentration distribution
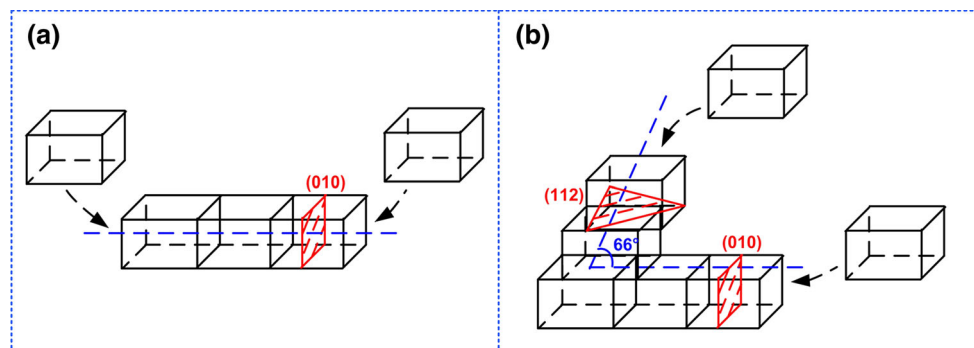

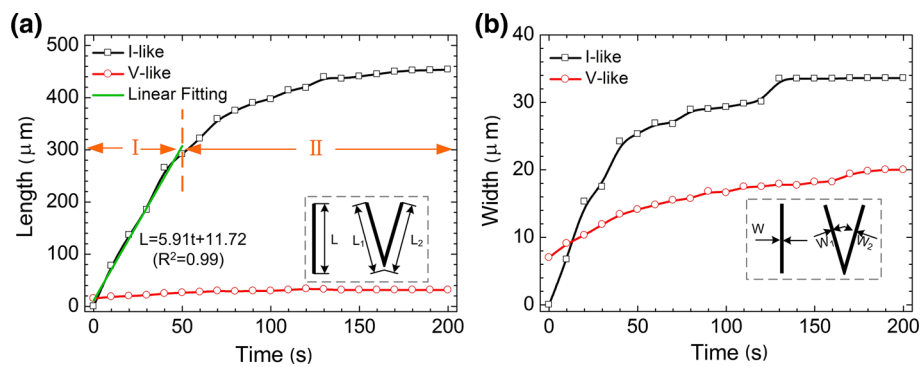**Fig. 4** Sketch of the I-like **a** and V-like **b** Al$_3$Ni phase growth

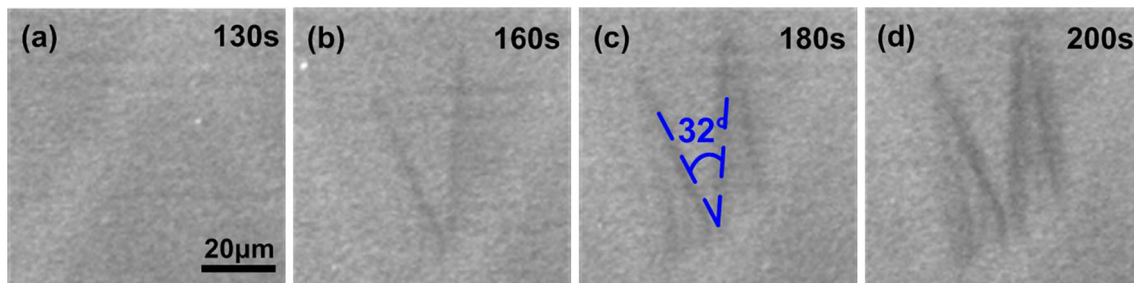Fig. 5 Time dependence of length **a** and width **b** of primary Al$_3$Ni phase

Fig. 6 Images at higher magnification of area that is marked by circle in Fig. 2i showing the formation of M-like Al$_3$Ni

around the M-like IMC to fully explain its growth behavior and evolution mechanism in the future.

4 Conclusion

In summary, the microstructural evolution in solidifying Al-10 wt% Ni alloy was directly observed by synchrotron radiography. Al$_3$Ni IMCs grow mainly in the form of I-like and V-like shapes during solidification, and it is energetically favorable that the I-like Al$_3$Ni phase grew faster than the V-like one. I-like Al$_3$Ni phase growth can be divided into two stages with a constant-decelerating growth mode, which is dominated by the variations of undercooling and Ni concentration.

References

[1] Y. Fukui, H. Okada, N. Kumazawa, Y. Watanabe, Metall. Mater. Trans. A **31**, 2627 (2000)
[2] P. Yu, C.J. Deng, N.G. Ma, D.H.L. Ng, J. Mater. Res. **19**, 1187 (2004)
[3] T.P.D. Rajan, R.M. Pillai, B.C. Pai, J. Alloys Compd. **453**, L4 (2008)
[4] M.V. Cante, J.E. Spinelli, N. Cheung, A. Garcia, Met. Mater. Int. **16**, 39 (2010)
[5] A. Juarez-Hernandez, H. Jones, Scr. Mater. **38**, 729 (1998)
[6] X. Li, Y. Fautrelle, A. Gagnoud, R. Moreau, D. Du, Z.M. Ren, X.G. Lu, Metall. Mater. Trans. A **47**, 1180 (2016)
[7] X. Li, Z.M. Ren, Y. Fautrelle, J. Cryst. Growth **310**, 3488 (2008)
[8] C.J. Wang, Q. Wang, Z.Y. Wang, H.T. Li, K.J. Nakajima, J.C. He, J. Cryst. Growth **310**, 1256 (2008)
[9] H.R. Shahverdi, M.R. Ghomashchi, S. Shabestari, J. Hejazi, J. Mater. Process. Technol. **124**, 345 (2002)
[10] X. Qiu, J. Wang, Scr. Mater. **56**, 1055 (2007)
[11] R. Chen, Q.Y. Xu, B.C. Liu, Acta Metall. Sin. (Engl. Lett.) **28**, 173–181 (2015)
[12] H.T. Ma, L. Qu, M.L. Huang, L.Y. Gu, N. Zhao, L. Wang, J. Alloys Compd. **537**, 286 (2012)
[13] M.L. Huang, F. Yang, N. Zhao, Z.J. Zhang, Mater. Lett. **139**, 42 (2015)
[14] C. Puncreobutr, A.B. Phillion, J.L. Fife, P. Rockett, A.P. Horsfield, P.D. Lee, Acta Mater. **79**, 292 (2014)
[15] Z.Y. Ding, Q.D. Hu, W.Q. Lu, S.Y. Sun, M.X. Xia, J.G. Li, Scr. Mater. **130**, 214 (2017)
[16] K. Morsi, Mater. Sci. Eng. A **299**, 1 (2001)
[17] H.X. Li, Y. Fautrelle, L. Hou, D.F. Du, Y.K. Zhang, Z.M. Ren, J. Cryst. Growth **436**, 68 (2016)
[18] A. Yamamoto, H. Tsubakino, Scr. Mater. **37**, 1721 (1997)
[19] T.M. Wang, P. Zhou, F. Cao, H.J. Kang, Z.N. Chen, Y.N. Fu, T.Q. Xiao, W.X. Huang, Q.X. Yuan, Intermetallics **58**, 84 (2015)
[20] W. Kurz, D.J. Fisher, *Fundamentals of Solidification*, 3rd edn. (Trans Tech Publications Ltd, Switzerland, 1992), pp. 22–28